Diffraction grating single-shot correlation system for measurement of picosecond laser pulses

Fuling Zhang (张福领)[1,2*], Xiaoping Ouyang (欧阳小平)[1], Meizhi Sun (孙美智)[1], Qunyu Bi (毕群玉)[1], Xinglong Xie (谢兴龙)[1], and Zunqi Lin (林尊琪)[1]

[1]*Shanghai Institute of Optics and Fine Mechanics, Chinese Academy of Sciences, Shanghai 201800, China*

[2]*The 27th Research Institute of China Electronics Technology Group Corporation, Zhengzhou 450015, China*

**E-mail: flzhang666@163.com*

Received April 2, 2010

We study and experimentally demonstrate a sensitive single-shot correlation system in which only a diffraction grating is used to produce a transverse time delay (TTD) in the reference pulse. The mechanism of the TTD introduced by the grating and the formation of the relative time delay (RTD) in the noncollinear correlation system are analyzed in detail. By using our system, we successfully measured the temporal duration of picosecond laser pulses, and a time resolution of ∼0.047 ps is obtained at 1047 nm. The impact of the grating dispersion and the second harmonic beam walk-off effect on the measurement are considered.

OCIS codes: 050.1950, 120.4640, 190.2620.

doi: 10.3788/COL20100811.1053.

Since the development of the mode-locked Nd:glass laser, a number of methods have been proposed to measure the duration of ultrashort laser pulses[1−7]. One of the methods to measure single ultrashort laser pulses is to use a commercial streak camera[1], which has the advantage of obtaining direct information of the pulse. However, it is too expensive to monitor the pulse in this way, and the time resolution is restricted to several picoseconds at present. As another method, two-photon fluorescence (TPF) technique has often been used to measure the picosecond laser pulses[2]. The TPF method has a time resolution of below picosecond, but it has a highly disturbing background signal, which does not allow weak pulses near the main pulse to be seen. Later, Gyuzalian *et al.* used a noncollinear second-harmonic generation (SHG) technique to transform the temporal shape of the pulse into a spatial shape which could be analyzed by a spatial detector[4,5]. Though this technique can offer very high temporal resolution, the long record temporal range of tens to hundreds of picoseconds is difficult to satisfy in single-shot correlation measurements since they require both very large nonlinear crystal apertures and large beam crossing angles. To complement this, Wyatt *et al.* have used an original method of measuring pulses of subnanosecond to picosecond duration, using a diffraction grating to produce a tailored, expanded beam with a differential time delay along its expanded axis[6]. However, the efficiency of the grating at grazing incidence is very low. In succession, Ross *et al.* proposed a technique for measuring the pulse duration of a single picosecond pulse at 249 nm by using a grating operating in the first order to introduce a variable delay across the beam, but the mechanism of the transverse time delay (TTD) introduced by the grating and the formation of the relative time delay (RTD) in the noncollinear correlation have not been fully explored[7].

In this letter, we study and experimentally demonstrate a single-shot correlation system in which a diffraction grating is used to produce a TTD in the reference pulse. The mechanism of the TTD introduced by the grating and the formation of the RTD in the noncollinear correlation system are analyzed in detail. To measure a wider range of pulse duration sensitively with a moderate-sized nonlinear crystal aperture, different grating, different incident angle, and different order of diffraction are suggested. In our system a low loss beam-expanding telescope is used to expand (if needed) the beam and a high efficiency diffraction grating is mainly used to introduce TTD. This results in a considerable increase of sensitivity and a wider duration measurement range with a moderate nonlinear crystal aperture size. By using this system, we successfully measure the temporal duration of picosecond pulses output from a Jaguar-QCW laser (Time Bandwidth Inc). The impact of the grating dispersion and the second harmonic (SH) beam walk-off effect on the measurement is also considered.

The basic idea of our method is to transform the temporal shape of the pulse into a spatial shape which could be analyzed by a spatial detector. The laser pulse entering into the correlation system is split into two beams by a beam splitter (BS); one beam is used to provide a reference pulse and the other beam is used to provide a signal pulse. A diffraction grating is used to produce a TTD in the reference pulse. A delay line is inserted in the path of the signal beam to ensure the temporal and spatial overlap of the two pulses in a nonlinear crystal. Then the two beams cross in the nonlinear crystal in order to generate a noncollinear SH signal, which is recorded by a linear array of charge-coupled device (CCD).

A standard diffraction grating is used to introduce a tilt in the pulse front with respect to the phase front which is perpendicular to the propagation direction, as shown in Fig. 1. The tilt of the pulse front causes a TTD across the spatial extent of the beam.

In this case, the grating equation is

$$d(\sin i + \sin \theta) = m\lambda, \quad (1)$$

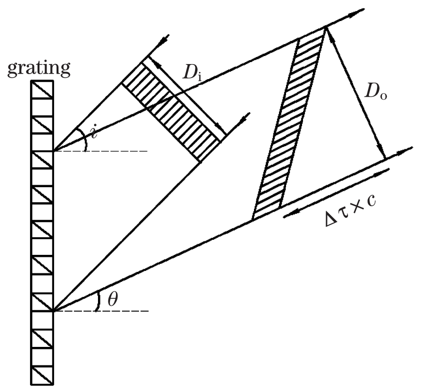

Fig. 1. Formation of the transverse time delay in a beam diffracted from a grating.

where d is the grating constant, i is the angle of incidence, θ is the angle of diffraction, m is the order of diffraction, and λ is the mean wavelength of the laser pulse. For this condition, we can deduce the total TTD across the beam with

$$\Delta\tau = \frac{m\lambda D_{\rm i}}{dc\cos i} = \frac{m\lambda D_{\rm o}}{dc\cos\theta}, \tag{2}$$

where $D_{\rm i}$ is the incident beam diameter, $D_{\rm o}$ is the output beam diameter, and c is the velocity of light in vacuum. Obviously, if we choose different grating with respect to the grating constant, different angle of incidence, and different order of diffraction, the total TTD across the beam in a very wide range can be obtained.

The transform-limited pulse diffracted by the grating becomes lengthened due to the temporal chirp. The general description of the effect of temporal chirp is based on the calculation of the phase of a light wave upon propagation. If the second derivative of the phase $\phi(\omega)$, that is, the group delay dispersion (GDD) is not zero, then the pulse is temporally chirped and, hence, lengthened. And GDD can be expressed as[8,9]

$$\mathrm{GDD} = \left.\frac{\mathrm{d}^2\phi}{\mathrm{d}\omega^2}\right|_{\omega_0} \approx -\frac{\omega_0\cdot L}{c}\left(\left.\frac{\mathrm{d}\theta'}{\mathrm{d}\omega}\right|_{\omega_0}\right)^2,$$

where L is the distance between the source of angular dispersion and the position of observation along the ray of the central frequency ω_0, and θ' is the angle between the rays of ω_0 and an arbitrary frequency ω. Assuming a transform-limited Gaussian input pulse, the length of the output pulse is

$$\tau_{\rm p}' = \tau_{\rm p}\sqrt{1+\left(\Delta\omega^2\frac{\mathrm{GDD}}{4\ln 2}\right)^2},$$

where $\Delta\omega$ is the full-width at half-maximum (FWHM) bandwidth of the pulse and $\tau_{\rm p}$ is the length of the input pulse. If a 12-ps, 1.047-μm pulse is diffracted by a 1200-l/mm grating, the length of the output pulse is about 12.0004 ps. The effect of pulse lengthening is too small to be considered. The longer the laser pulse is, the smaller the magnitude of pulse lengthening is. Thus, the dispersive pulse stretching can be neglected for tens of picoseconds laser pulses.

We use Fig. 2 to obtain the intensity of the SH signal produced at a distance x from the center of the SH beam. Let $I_1(t)$ and $I_2(t)$ be the temporal intensity shapes of the incident pulses and $S(x)$ be the spatial shape of the SH signal. As the detector integrates the SH signal over a longer time than the pulse width, we finally obtain a shape $S(x)$ proportional to the second-order correlation function $G_2(\tau)$ of the incident pulse:

$$\begin{aligned} S(x) &\propto \int_{-\infty}^{+\infty} I_1(t-\tau-\tau')I_2(t+\tau)\mathrm{d}t \\ &= \int_{-\infty}^{+\infty} I_1[t'-(2\tau+\tau')]I_2(t')\mathrm{d}t' = G_2(2\tau+\tau'), \end{aligned} \tag{3}$$

where

$$\tau = \frac{nx\sin\phi}{c} \quad \text{(RTD from crossing interaction)}, \tag{4}$$

$$\tau' = \frac{\Delta\tau\cdot x\cos\phi}{D_o} = \frac{m\lambda x\cos\phi}{dc\sqrt{1-(m\lambda/d-\sin i)^2}}$$
$$\text{(RTD from diffraction grating)}, \tag{5}$$

and 2ϕ is the crossing angle of the two incident beams in the crystal.

Obviously, both the crossing interaction and the diffraction grating can be used to introduce RTD. As can be seen from Fig. 3, if the beam diameter is large enough, the RTD is in direct proportion with the crystal aperture, and the RTD due to crossing interaction is much smaller than that from diffraction grating for the same nonlinear crystal aperture size. So we can say that the crossing interaction is mainly used to ensure background-free measurement and the grating is primarily used to introduce RTD. Figure 4 is given by calculating the RTD introduced by gratings for a certain crystal aperture size. It is shown that, to measuring broader pulses, one should use gratings with smaller grating constant and smaller incident angle for a moderate nonlinear crystal aperture size.

The experimental setup is schematically shown in Fig. 5. We use a Jaguar-QCW laser that produces about 12-ps, 500-μJ pulses at 1047 nm with 10-Hz recurrence. The output beam of the laser is properly expanded and collimated before it enters the pulse correlation system to ensure that the spatial intensity profile of the pulse is uniform across the crystal aperture. The laser pulse entering into the system is split into two beams by a BS; one beam is used to provide a reference pulse and the other beam is used to provide a signal pulse. The reference pulse impinges on a diffraction grating of 1200 l/mm,

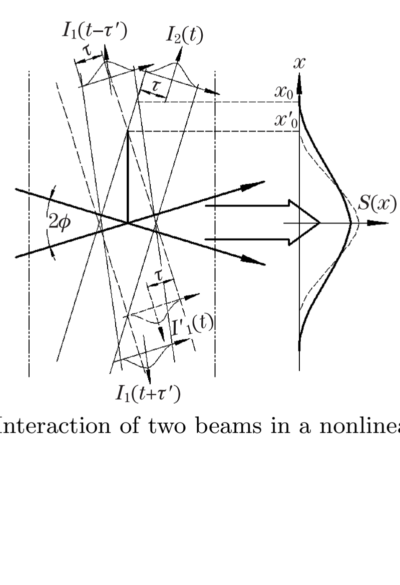

Fig. 2. Interaction of two beams in a nonlinear crystal.

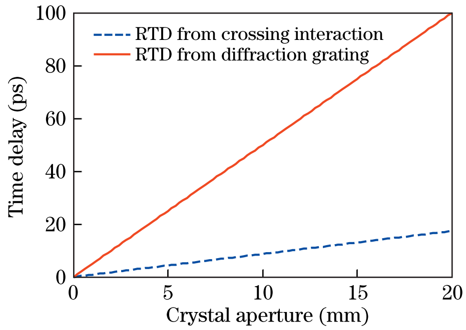

Fig. 3. Calculated RTD as a function of crystal aperture for different sources.

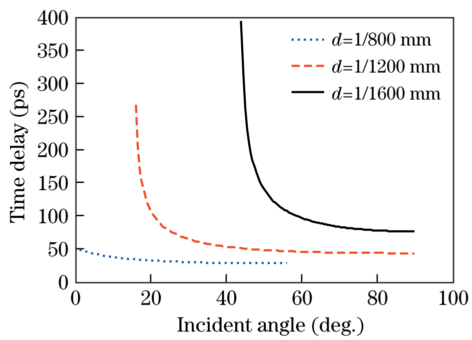

Fig. 4. Calculated RTD introduced by different gratings.

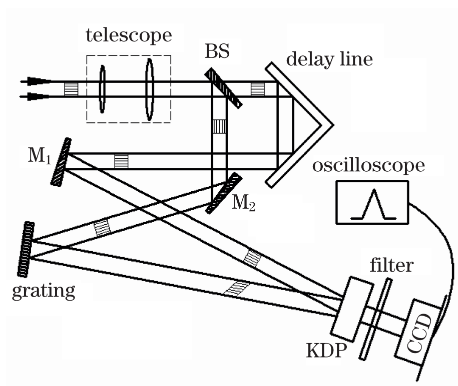

Fig. 5. Experimental setup of the correlation system.

and the incident angle is set to $\sim 45°$, resulting in a diffraction efficiency of $\sim 80\%$ in the first order. A delay line is inserted in the path of the signal beam to ensure the temporal and spatial overlap of the two pulses in a nonlinear crystal (KDP). The crystal cut (44.5°) and the crystal orientation are designed to satisfy the type I phase-matching condition for noncollinear SHG. The crossing angle of the two beams is set to $\sim 14°$ in the crystal, although this angle is not critical. A BG18 filter selects the signal at 524 nm and stops the incident pulses at 1047 nm. The spatial distribution of the noncollinear SH signal is recorded by a linear array of CCD, and finally displayed on an oscilloscope screen.

In out measurement, we need to calibrate the scale of the time-to-space conversion. Calibration is performed by introduction of a known time delay Δt into the signal pulse and measurement of the transverse spatial displacement Δx of the SH signal. The width (FWHM) L_x of the spatial function $S(x)$ is connected with the FWHM t_p of the SH signal pulse by[5]

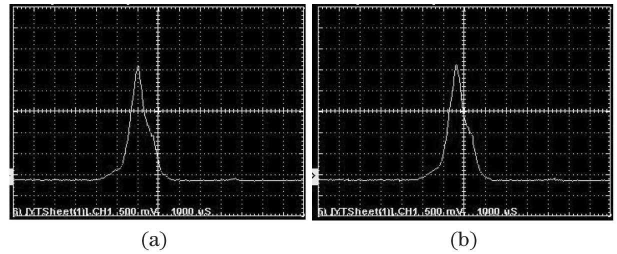

Fig. 6. Single-shot correlation curves on the oscilloscope (a) before and (b) after a time delay Δt =14.467 ps is introduced.

$$t_p = \frac{L_x}{K} \cdot \frac{\Delta t}{\Delta x}, \tag{6}$$

where K is a form factor depending on the incident pulse shape (K=1.543 for a sech^2 pulse, K=1.414 for a Gaussian pulse)[10].

A micrometer with a resolution of 0.01 mm (corresponding to $\sim$ 33 fs in vacuum) is used to introduce a precise time delay Δt into the signal pulse. As shown in Fig. 6, when we introduce a time delay Δt = 14.467 ps into the signal pulse, the peak of the SH signal moves Δx = 680 μs. So we obtain the calibration factor $\Delta t/\Delta x$ = 21.275 fs/μs. The FWHM of a typical recorded SH signal profile on the oscilloscope screen is measured as L_x= 800 μs, which corresponds to an actual pulse duration of $\sim$11.03 ps, assuming a sech^2 pulse shape. This single-shot measurement is in good agreement with pulse width determination carried out previously ($\sim$ 11.34 ps).

As pointed out before, using different grating with respect to the grating constant, different angle of incidence, and different order of diffraction, pulse duration in a very wide range can be measured without an unduly large nonlinear crystal aperture size. For shorter pulses, the main limitation will arise from the walk-off effect in the nonlinear crystal. In uniaxial crystals, there exists a walk-off angle α between the k-vector and the Pointing vector of the extraordinary beam. For an interaction length l, this angle leads to a broadening of the SH beam of $\Delta z = l \times \sin\alpha$. In our experiment, we work with a KDP with thickness of l = 2 mm, crossing angle $2\phi \approx 14°$, phase matching angle $\theta \approx 16°$, and walk-off angle $\alpha \approx 0.88°$. The SH beam broadening of $\Delta z \approx 0.03$ mm corresponds to a reduced accuracy in the full pulse duration of $\sim$ 0.1 ps.

The beam diffracted by the grating becomes divergent due to the finite spectral bandwidth and the angular dispersion. This divergence may influence the process of SHG in the nonlinear crystal and should be taken into account. Assuming a Gaussian-shaped pulse of a time duration $\tau_{\rm p}$, it is easy to calculate the divergence of the beam in the plane of incidence, which is due to dispersion[11]

$$\Delta\theta_{\rm disp} = 0.44\frac{\lambda^2}{cd\tau_{\rm p}}. \tag{7}$$

Equation (7) may help the evaluation of the divergence due to the diffraction grating. For example, if the pulse width is 12 ps at 1.047-μm wavelength and we use a 1200-l/mm grating, the divergence is only about 0.5788 arcsec. This value is acceptable for most available nonlinear crystals. The shorter the laser pulse, the wider the spectral bandwidth, and the higher the divergence. Thus, the divergence due to dispersion can be kept low if one employs gratings with constant d inversely proportional to the pulse width.

The temporal resolution for 2-mm KDP limited by the group velocity dispersion is calculated to be 6.77 fs at 1047 nm. The CCD we used consists of 4096 pieces of active elements with a dimension of 10×10 (μm). This spatial resolution provides a temporal resolution of 33 fs. So a temporal resolution of ~ 0.047 ps for our system is determined by considering the dispersion in KDP, the CCD spatial resolution, and a time-based calibration.

In conclusion, we have studied and demonstrated experimentally a sensitive single-shot pulse correlation system in which a diffraction grating is used to produce a TTD in the reference pulse. The mechanism of the TTD introduced by the grating and the formation of the RTD in the noncollinear correlation system are analyzed in detail. The crossing interaction is mainly used to ensure background-free measurement and the diffraction grating is primarily used to introduce RTD in our noncollinear correlation system. And the pulse duration measurement coverage can be extended by employing appropriate grating, incident angle, and order of diffraction. So this system can be used to produce sensitive background-free correlation function for a single incident pulse in a wide duration coverage without an unduly large nonlinear crystal aperture. By using this system, we successfully measure the temporal duration of picosecond laser pulses, and a time resolution of ~ 0.047 ps is obtained at 1047 nm. This system can also be used to optimize the alignment of our optical parametric chirped pulse amplification (OPCPA) grating compressor.

This work was supported by the National "863" Program of China under Grant No. 2009AA8044010.

References

1. D. J. Bradley, B. Liddy, and W. E. Sleat, Opt. Commun. **2,** 391 (1971).
2. J. A. Giordmaine, P. M. Rentzepis, S. L. Shapiro, and K. W. Wecht, Appl. Phys. Lett. **11,** 216 (1967).
3. X. Ouyang, F. Zhang, P. Zhang, X. Xie, and J. Zhu, Chinese J. Lasers (in Chinese) **36,** 742 (2009).
4. R. N. Gyuzalian, S. B. Sogomonian, and Z. Gy. Horvath, Opt. Commun. **29,** 239 (1979).
5. F. Salin, P. Georges, G. Roger, and A. Brun, Appl. Opt. **26,** 4528 (1987).
6. R. Wyatt and E. E. Marinero, Appl. Phys. **25,** 297 (1981).
7. I. N. Ross, D. Karadia, and J. M. Barr, Appl. Opt. **28,** 4054 (1989).
8. K. Osvay, A. P. Kovács, Z. Heiner, G. Kurdi, J. Klebniczki, and M. Csatári, IEEE J. Sel. Top. Quantum Electron. **10,** 213 (2004).
9. Q. Yang, A. Guo, X. Xie, F. Zhang, M. Sun, Q. Gao, M. Li, and Z. Lin, Chinese J. Lasers (in Chinese) **35,** 1970 (2008).
10. J.-C. M. Diels, J. J. Fontaine, I. C. McMichael, and F. Simoni, Appl. Opt. **24,** 1270 (1985).
11. S. M. Saltiel and K. A. Stankov, Appl. Phys. B **35,** 45 (1984).